Functional Role of Conserved Transmembrane Segment 1 Residues in Human Sodium-Dependent Vitamin C Transporters[†]

Saaket Varma,[‡] Christine E. Campbell,[‡] and Shiu-Ming Kuo*[,‡,§]

Department of Biochemistry and Department of Exercise and Nutrition Sciences, University at Buffalo, Buffalo, New York 14214

Received August 17, 2007; Revised Manuscript Received January 2, 2008

ABSTRACT: Sodium-dependent vitamin C transporters, SVCT1 and SVCT2, are the only two known proteins for the uptake of ascorbate, the active form of vitamin C. Little structural information is available for SVCTs, although a transport activity increase from pH 5.5 to 7.5 suggests a functional role of one or more conserved histidines ($pK_a \approx 6.5$). Confocal fluorescence microscopy and uptake kinetic analyses were used here to characterize cells transfected with mutants of EGFP-tagged hSVCTs. Mutating any of the four conserved histidine residues (His51, 147, 210, or 354) in hSVCT1 to alanine did not affect the apical membrane localization in polarized MDCK cells. His51Ala (in putative transmembrane segment 1, TM1) was the only mutation that resulted in a significant loss of ascorbate transport and an increase in apparent *K*m with no significant effect on *V*max. The corresponding mutation in hSVCT2, His109Ala, also led to a loss of transport activity. Among eight other mutations of His51 in hSVCT1, significant sodium-dependent ascorbate transport activity was only observed with asparagine or tyrosine replacement. Thus, our results suggest that uncharged His51, directly or indirectly, contributes to substrate binding through the hydrogen bond. His51 cannot account for the observed pH dependence as neutral amino acid substitutions failed to abolish the pH-dependent activity increase. The importance of TM1 is further strengthened by the comparable loss of sodium-dependent ascorbate transport activity upon the mutation of adjacent conserved Gln50 and the apparent change in substrate specificity in the hSVCT1-His51Gln mutation, which showed a specific increase in sodium-independent dehydroascorbate transport.

Scurvy, as a life-threatening clinical manifestation of vitamin C deficiency, first demonstrated the essential role of vitamin C in human health. Sodium-dependent vitamin C transporters, SVCT1 and SVCT2, were found to be the only two functional proteins in humans for transporting the active form of vitamin C, ascorbic acid, into the cells (for a review, see ref *1*). The more hydrophobic oxidized form of vitamin C, dehydroascorbate (reviewed in ref *1*) is believed to be transported by facilitated glucose transporters (reviewed in ref *2*). Although there are no animal models of SVCT1 deficiency, SVCT2 knockout mice exhibit perinatal lethality (*3*), demonstrating the importance of this latter protein for viability. Also, a recent population study suggested that genetic polymorphisms in both SVCT1 and SVCT2 are risk factors for preterm delivery (*4*). In contrast to the extensive physiological information on vitamin C transport, there is little information on the amino acid residues that are crucial for the structure/function of SVCTs. Our research presented here defines the importance of two evolutionarily conserved amino acid residues in the first putative transmembrane segment (TM[1]) of SVCTs.

Human SVCT1 and SVCT2 are 66% identical, and their homology is higher in the putative 12 TM regions than in the putative intracellular and extracellular domains. Both transporters exhibit physiologically relevant affinity for L-ascorbic acid (*K*m in the 10^{-5} to 10^{-4} M range) (reviewed in refs *1* and *5*). The proteins are unlikely to be functionally redundant, on the basis of the lethality of SVCT2 null mutations in mice (*3*), as well as the observation that SVCT1 and SVCT2 appear to have different tissue and subcellular distributions (*1, 6, 7*). SVCT2 is ubiquitously expressed, while SVCT1 is primarily restricted to intestine, kidney, and other epithelial cells (*1, 8*). Exogeneously expressed hSVCT1-EGFP and hSVCT2-EGFP localize to the apical and basolateral membranes of polarized kidney or intestinal epithelial cells, respectively (*6, 7*).

Histidine residues have been shown to influence the substrate affinity (*9–11*) and pH-dependent activity change (*11–14*) of membrane proteins. Higher sodium-dependent accumulation of vitamin C was observed at buffer pH 7.5 than at pH 5.5 in human intestinal brush border membrane vesicles (*15*). Similarly, exogenously introduced SVCTs exhibit higher activities and apparent ascorbate affinities as pH increases from 5.5 to 7.5 (*1, 16*). This pH-dependence profile has led to the suggestion that one or more conserved histidine residues may be involved in the transport activity of SVCTs (*16*) since the imidazolium group of histidine has

[†] This work was supported partly by UB Mark Diamond Research Fund (to S.V.).

* To whom correspondence should be addressed. Tel: 716-829-3680. Fax: 716-829-3700. E-mail: smkuo@buffalo.edu.

[‡] Department of Biochemistry.

[§] Department of Exercise and Nutrition Sciences.

[1] Abbreviations: AsA, ascorbate; CHO, Chinese hamster ovary; DHA, dehydroascorbate; DTT, dithiothreitol; MDCK, Madin-Darby canine kidney; NMG, *N*-methylglucamine; hSVCT, human sodium-dependent vitamin C transporter; TM, transmembrane segment.

10.1021/bi701666q CCC: $40.75 © 2008 American Chemical Society
Published on Web 02/05/2008

Table 1: Sequences of Forward Primers Used for the Mutagenesis of SVCT[a]

mutant	forward primer
SVCT1	
H51A(QA)	5′-CATCCTGCTGGGCTTCCAGGCTTACCTGACATGCTTC-3′
H147A	5′-GCCCCTGAACACCTCTGCTATTTGGCACCCACGGATAC-3′
H210A	5′-GCGACCGAGCTGGCTCCGCCTGGGGCATCTCAG-3′
H354A	5′-GCACCACCCCCTCCAGTAGCCGCTATCAACAGG-3′
H51C(QC)	5′-CATCCTGCTGGGCTTCCAGTGCTACCTGACATGCTTCA-3′
H51D(QD)	5′-CATCCTGCTGGGCTTCCAAGACTACCTGACATGCTTCA-3′
H51E(QE)	5′-CATCCTGCTGGGCTTCCAAGAATACCTGACATGCTTCA-3′
H51K(QK)	5′-CATCCTGCTGGGCTTCCAGAAATACCTGACATGCTTCA-3′
H51N(QN)	5′-CATCCTGCTGGGCTTCCAGAACTACCTGACATGCTTCA-3′
H51Q(QQ)	5′-CATCCTGCTGGGCTTCCAGCAATACCTGACATGCTTCA-3′
H51R(QR)	5′-CATCCTGCTGGGCTTCCAGCGTTACCTGACATGCTTCA-3′
H51Y(QY)	5′-CATCCTGCTGGGCTTCCAATACTACCTGACATGCTTCA-3′
Q50A(AH)	5′-CATCCTGCTGGGCTTCGCTCACTACCTGACATGCTTCA-3′
Q50H,H51Q(HQ)	5′-CATCCTGCTGGGCTTCCACCAATACCTGACATGCTTCA-3′
SVCT2	
H109A	5′-CTGGGGCTACAGGCGTACCTGACATGCTTCAGCGG-3′

[a] Underlined letters represent the nucleotides that have been changed to achieve the desired mutations. Complementary sequences were used as the reverse primers.

a $pK_a \approx 6.5$. To address the potential role of histidine residues in substrate binding and pH dependence of transport, we utilized two vectors encoding EGFP-tagged hSVCT1 and hSVCT2, originally constructed and characterized in this laboratory (*6*). EGFP-tagging has been used in studies of membrane transporters previously (*14, 17–19*). Because a similar pH dependence of transport activity was observed for both hSVCT1 and hSVCT2, we focused our single amino acid mutation analysis on the four conserved histidines present in both proteins across several mammalian species (*16*).

On the basis of our results from membrane localization and uptake kinetic analyses, we propose a substrate-binding role of the conserved histidine in the first TM of hSVCTs. In addition, the adjacent conserved glutamine in TM1 is also critical for the function of hSVCT1.

EXPERIMENTAL PROCEDURES

Materials. L-[Carboxyl-^{14}C]ascorbic acid (13 mCi/mmol) was purchased from Amersham Biosciences (Buckingshire, England). [^{14}C(U)]-L-phenylalanine (360 mCi/mmol) and [^{14}C(U)]-2-deoxy-D-glucose (303 mCi/mmol) were from Moravek Biochemicals Inc. (Brea, CA) L-ascorbic acid (SigmaUltra) was from Sigma Aldrich (St. Louis, MO). Dehydroascorbic acid was from Fluka (Milwaukee, WI). All cell culture reagents were from Invitrogen Corp. (Carlsbad, CA) except for characterized fetal bovine serum, which was purchased from Hyclone, USA (Logan, UT). All other chemicals used were of reagent grade. Primers used for the site-directed mutagenesis and for the sequencing were from Operon Biotechnologies, Inc. (Huntsville, AL) (Table 1).

Plasmid Preparation and the Generation of Mutant-Expressing Stable Cell Lines. QuikChange Site-Directed Mutagenesis Kit from Stratagene (La Jolla, CA) was used to create point mutations in the hSVCT1-EGFP and hSVCT2-EGFP plasmids previously generated in this laboratory (*6*). Plasmids were purified using Perfectprep Plasmid kits (Eppendorf, Hamburg, Germany) and sequenced. A calcium phosphate-mediated transfection protocol was used to introduce the mutant plasmids into MDCK and CHO cells (*6*). CHO cells are a model of nonpolarizing epithelial cells; therefore, we can measure the uptake of hSVCT2 in 6-well plates in contrast to the Transwell apparatus for MDCK cells. Stable cell lines were generated using G418 selection and maintained in high-glucose Dulbcco's modified Eagle media (Invitrogen) supplemented with 200 μg/mL G418 as described previously (*6*). To confirm the fidelity of the mutations within the transfectants, genomic DNA was extracted from stable cell lines (MasterPure DNA Purification Kit, Epicenter, Madison, WI) and subjected to PCR to amplify the mutated region. PCR products were gel purified (QIAquick Gel Extraction Kit, Qiagen, Inc. Valendia, CA) and sequenced. All sequencing was performed by the facility at Roswell Park Cancer Institute (Buffalo, NY). The mutant cell lines are named on the basis of the standard nomenclature of mutant proteins. All experiments were performed on 12–16 day cultures of early passages of cell lines stably expressing the various plasmids.

Uptake Assays and Data Analysis. Ascorbate uptake assays were performed on cells grown in 6-well plates incubated in HEPES and penicillin−streptomycin-supplemented Hanks' balanced salt solution (Invitrogen) containing L-[carboxyl-^{14}C]ascorbic acid. Assays were carried out at 37 °C at pH 7 following our previously described protocol (*6, 20, 21*). Briefly, a reducing agent, 0.1 mM dithiothreitol (DTT), was included in the uptake buffer to prevent the oxidation of ascorbate (*22*). *N*-Methylglucamine (NMG) at 135 mM was substituted for sodium in the preparation of Hanks' balanced salt solution without sodium. The pH adjustment of Hanks' solution was carried out with 1 N KOH or HCl solutions. On the basis of spectra absorption analyses, ascorbate is stable within the pH range of 6.5 to 8 in our experimental buffer with no loss of absorbance peak at 266 nm after a 15-min incubation at 37 °C. Higher pH values led to the loss of the 266 nm peak under otherwise identical experimental conditions. Thus, the transport activity was tested within the pH range of 6.5 to 8. With the exception of the kinetic analysis experiments, the concentration of ascorbate in the uptake solution was 10 μM or 40 μM (physiologically relevant concentrations) as indicated in the figure legends, with total radioactivity in each well ~0.03 μCi. Because the sodium-dependent vitamin C transport activity was not affected by the presence of DTT (see Results section Figures 4 and 6), kinetic analyses were performed at pH 7 in the absence of DTT. *K*m and *V*max values were calculated from

intercepts obtained from the linear regression of 1/*v* versus 1/[S] plots. Transwell uptake assays were also performed as described previously (*6*) to determine the uptake of vitamin C from the basolateral membrane by SVCT2. Uptake of ^{14}C-dehydroascorbate was determined following the published protocol from this laboratory (*23*). The stability of dehydroascorbate was determined by measuring the 2,4-dinitrophenylhydrazine derivative (*24*) after a 15 min incubation at 37 °C, mimicking the uptake experimental conditions.

Total protein content was determined by a modified Lowry assay with SDS using bovine serum albumin as the standard (*25*). All transport activity measurements were done in triplicate wells, and the means and standard deviations of the three independent wells are shown. Most experiments were repeated at least once. Data were analyzed by one-way ANOVA using StatView 4.01 as indicated in the figure legends. Posthoc Student–Newman–Keuls or Bonferroni/Dunn (compared to the control) multiple comparison was performed only if a significant main effect was detected.

Confocal Fluorescence Microscopy and Total Fluorescence Measurement. Postconfluent MDCK cells (12–16 days after seeding) used for imaging experiments were grown in Laboratory-Tek II chambered cover glasses (Nalge Nunc International Naperville, IL) as described previously (*6*). Images were captured in the Confocal and 3-D Imaging Core Facility of University at Buffalo. Because these analyses were carried out over a period of three years as different mutants were generated, some variations existed in the instrument parameters among different imaging sessions. Initially, a Nikon Diaphot fluorescence microscope was used as a part of the Bio-Rad MRC-1024 laser confocal microscope system. The confocal images were acquired within an enclosed 37 °C chamber with a Nikon 60× NA 1.4 objective, and a 488 nm laser line for excitation was used with an emission band-pass filter of 522 ± 16 nm. In later experiments, a Zeiss LSM510 Meta system was used in conjunction with a Pecon 37 °C Heating Insert, Zeiss 63× NA1.4 objective with 488 nm excitation laser line and band-pass emission filter of 500–550 nm. Nikon images were processed with Velocity LE 2.6 (Improvision, Inc. Lexington, MA), and Zeiss images were processed with Velocity LE 2.6 or LE 3.7. Multiple confocal images were collected from different areas of the slide chamber for each cell line, and representative images are shown. No adjustments of brightness, contrast, sharpness, and so forth were made to any of the acquired images. Total fluorescence emission from various lines of cells grown in the 96-well plates was measured using Biotek Synergy HT Multi-Detection Microplate Reader with excitation at 485/20 nm and emission at 528/20 nm in the presence of Ca,Mg-containing PBS.

RESULTS

Analyses of hSVCT Histidine Mutants. Through the sequence alignment of SVCT1 and SVCT2 from human, rat, and mouse (*16*), we identified four conserved histidine residues that are also present in the predicted canine sequences (GenBank XP_535207 and XP_534357). The published computer-assisted topology predictions of 12 TMs have consistently positioned the first and third histidines within TM1 and TM5 of SVCTs, respectively, while the predicted position of the second and fourth histidines differed between two publications (*16, 26*). Figure 1 illustrates the predicted location of these four histidines on the basis of the alignment of six sequences (SVCT1 and SVCT2 from human, rat, and mouse (*16*)). There are no other conserved histidines in the SVCTs. In hSVCT1, the mutation of these four histidines individually to alanine does not affect the predominantly apical membrane localization in MDCK cells (Figure 2A comparing SVCT1-EGFP to the mutants). We conclude from this result that none of the four histidines are essential for either membrane localization or specific apical membrane targeting of hSVCT1.

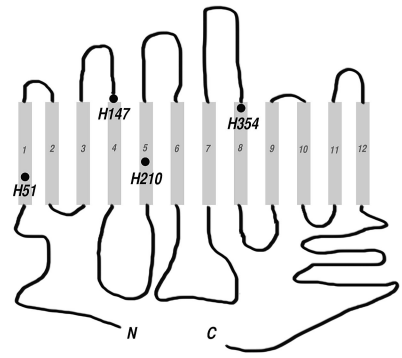

FIGURE 1: Predicted location of the four conserved histidine residues in the 12 TM of sodium-dependent vitamin C transporters (*16*). (●) conserved histidine. The residue numbering of histidines is based on hSVCT1. H109 in hSVCT2 corresponds to H51 in hSVCT1.

We then determined the sodium-dependent vitamin C transport activity of cell lines expressing these mutant proteins and their apparent *K*m and *V*max values. The results are shown in Figure 2B. Transport activities similar to the wild type hSVCT1-EGFP were observed in cells expressing hSVCT1-EGFP with His147Ala, His210Ala, or His354Ala mutation. In contrast, cells expressing the His51Ala mutant protein showed a 6-fold reduction in activity, a 6-fold increase in the apparent *K*m for ascorbate, and insignificant change in *V*max under the experimental conditions (Figure 2B). While variations in the expression efficiency of mutants can affect the net transport activities and hence apparent *V*max values, as a kinetic parameter, *K*m, is independent of protein concentration. We thus continued our study with a focus on His51 in TM1.

Since this TM1 histidine is also conserved in the SVCT2 protein, we measured the effect of mutating the corresponding residue (His109) in hSVCT2. Similar to wild type hSVCT2 (*6*), hSVCT2-H109A localized to the basolateral membrane of polarizing MDCK cells and the cell membrane of nonpolarizing CHO cells (Figure 3A). For both cell types, mutation led to a complete loss of sodium-dependent ascorbate transport activity (Figure 3B and C). The conserved histidine in TM1 thus appears to be equally crucial for hSVCT2.

After establishing the importance of TM1 histidine in sodium-dependent ascorbate transport activity (Figures 2 and 3), we conducted additional experiments to explore the possible function of this histidine. As the adjacent Gln50 is equally conserved on the basis of multiple protein sequence alignment (*16*), Gln50 has also been targeted in this study (see below) and is included as part of our mutant nomenclature. Figure 4 summarizes localization and activity measurements of eight additional hSVCT1 His51 mutants

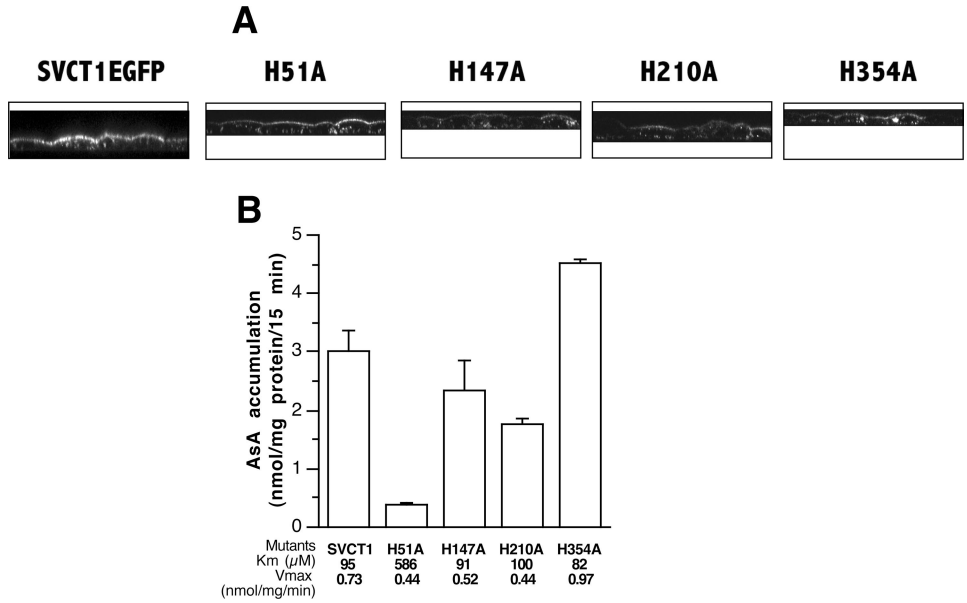

FIGURE 2: Comparison between wildtype SVCT1 and four SVCT1 mutants with single histidine to alanine point mutations, H51A, H147A, H210A, and H354A. (A) Apical membrane localization. (B) Sodium-dependent transport of ascorbate (at 40 μM ascorbate and 135 mM sodium) and apparent *K*m and *V*max for ascorbate. The transport activity of each group/experimental condition was measured in three independent wells of cells and is shown as mean ± SD.

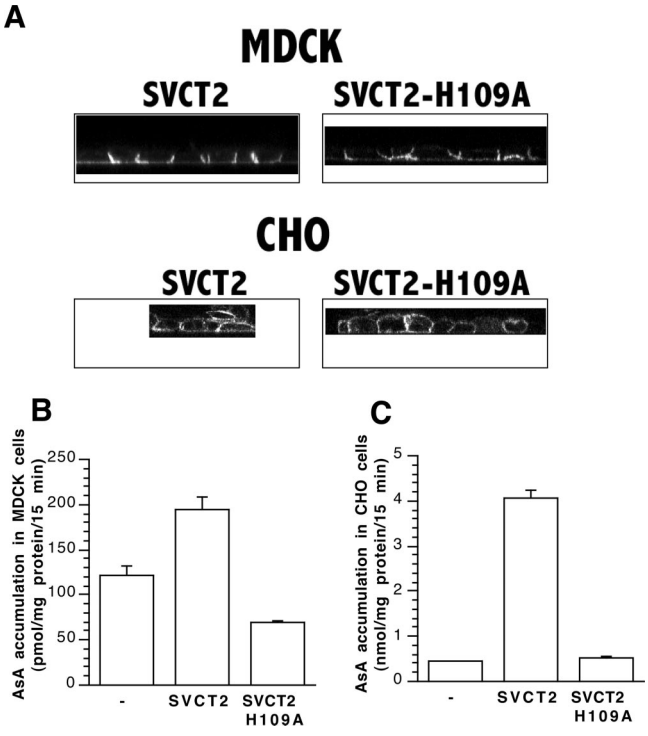

FIGURE 3: Effect of H109A mutation in SVCT2. (A) Confocal images showing the basolateral localization of wild type SVCT2 and SVCT2H109A mutant in MDCK cells and their cell membrane localization in CHO cells. Transport activities (at 10 μM ascorbate and 135 mM sodium) of nontransfected cells (-) and SVCT2- and SVCT2H109A-expressing cells were measured in (B) MDCK cells and (C) CHO cells. Three independent Transwells (uptake from the basolateral chamber) were used for each line of MDCK cells, and three independent wells of cells were used for CHO cells. Transwell data for SVCT2 in MDCK were from ref *6*. Data are expressed as the means ± SD. Some error bars are too small to be visible.

with QH being the wild type SVCT1. None of the histidine replacements, including those that introduced a negative (QD, QE) or positive (QK, QR) charge, disturbed the predominantly apical membrane expression of the protein (Figure 4A). Gross perturbation of protein structure or localization thus cannot account for the >80% activity loss observed in many of the mutants as shown in Figure 4B with untransfected MDCK cells (-) included as a negative control. Since DTT had no significant effect on the apparent transport activity of any mutant (Figure 4B), the stability of ascorbate in the buffer is thus not a factor for the activity difference among mutants.

Among the eight additional His51 mutants, considerable sodium-dependent ascorbate transport activity was observed in His51Asn (QN) and His51Tyr (QY) (Figure 4B). Both mutants, similar to His51Ala (QA), displayed increased apparent *K*m compared to that of the wild type with no significant changes in *V*max (Figure 4B). While the order of apparent activity was QH > QY > QN > QA, the order of apparent *K*m was QH < QY < QN < QA. Both Asn and Tyr can hydrogen bond and are uncharged, while Tyr also has a ring similarly planar to that of His.

pH Dependency of Sodium-Dependent Ascorbate Transport Activity of SVCT1 Histidine Mutants. The results in Figure 4 raised the question whether mutating His51 affected the previously described pH dependency of SVCT1 (*15, 16*). Increased sodium-dependent vitamin C transport activity was observed with increasing pH in wild type hSVCT1 and mutants (Figure 5A and B) including those with side chains that do not undergo pH-dependent changes in protonation (QA and QQ). QC, QQ, and QK mutants showed low activities similar to the untransfected MDCK cells at all pH values tested (Figure 5A). On the basis of the data in Figure 5A and B, His51 by itself is unlikely to play a critical role in the observed pH dependence of hSVCT1.

TM1 Glutamine Mutants of SVCT1. Since both residues, Gln50 and His51, are conserved across the species among SVCT family members (*16*), two hSVCT1 mutants, AH and HQ, were constructed to test the effect of mutating Gln50 on ascorbate transport activity. The results are shown in Figure 6. Neither mutation affected the predominantly apical

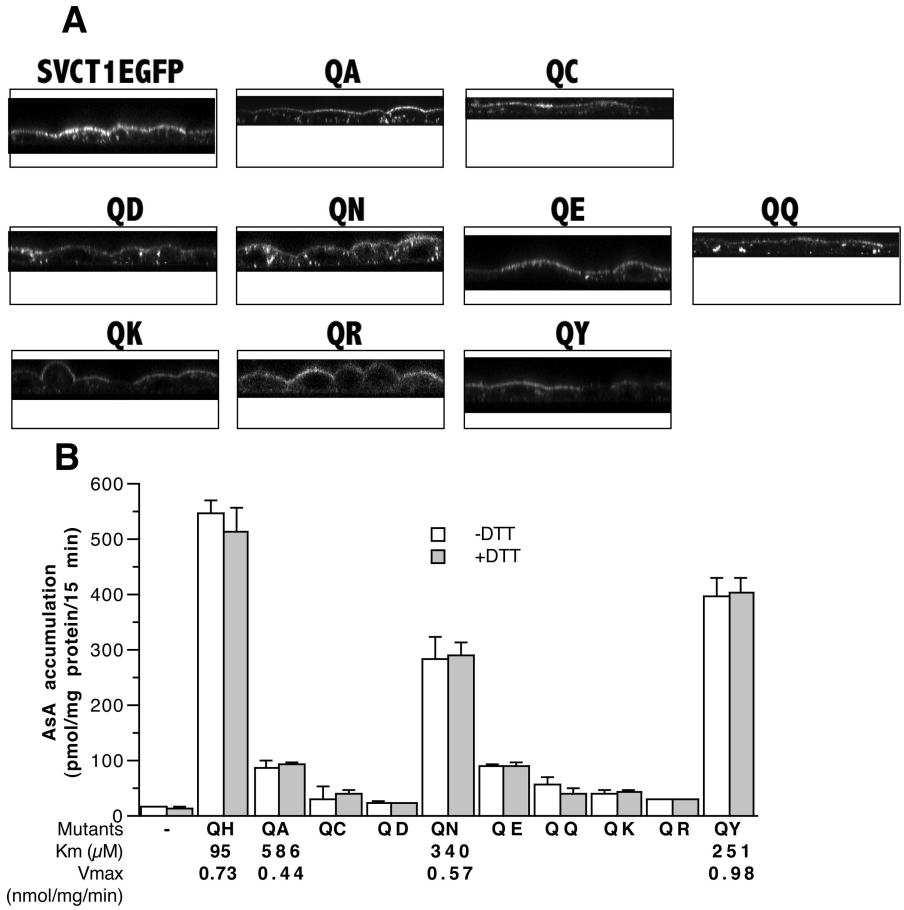

FIGURE 4: Characterization of various SVCT1 His51 mutants. (A) Apical membrane localization. (B) Net sodium-dependent ascorbate transport activity (at 10 μM ascorbate and 135 mM sodium) in the absence and presence of DTT and the *K*m and *V*max for ascorbate measured in the absence of DTT. The net sodium-dependent ascorbate transport activity was calculated by subtracting the activity measured in the absence of sodium from that measured in the presence of 135 mM sodium. -, nontransfected MDCK cells; QH, MDCK cells transfected with wildtype SVCT1. Other lanes represent measurements from MDCK cells transfected with mutant SVCT1 with the corresponding amino acid residue substituting for His51. The transport activity of each group was measured in three independent wells of cells and is shown as the mean ± SD. Some error bars are too small to be visible. The *K*m and *V*max values for QH and QA are from the same experiments as those for the SVCT1 and H51A in Figure 2B. The bar graphs and kinetic analyses represent the results from separate experiments.

localization of hSVCT1 (Figure 6A). The Gln50Ala (AH) mutant showed a 7-fold reduction in transport activity, while the HQ mutant with the order of the conserved residues switched had a complete loss of sodium-dependent ascorbate transport activity compared to that of the untransfected MDCK cells (labeled as -) (Figure 6B). Reducing agent DTT, again, has no effect on transport activities (Figure 6B, comparing the open with the filled bars), indicating that ascorbate oxidation cannot explain the activity loss of the mutants. The conserved Gln50 also appears critical for the sodium-dependent ascorbate transport of hSVCT1.

Sodium-Independent Dehydroascorbate Transport Activity of SVCT1 Mutants. Sodium-independent transport of ascorbate and dehydroascorbate in various hSVCT1 mutants was also measured to ask whether mutations in Gln50 or His51 affected the substrate specificity (Figure 7). Most mutants showed limited sodium-independent transport activities of ascorbate or dehydroascorbate similar to those of the hSVCT1 wild type (QH) or nontransfected MDCK cells (labeled as -) (Figure 7). The two mutants that have substantial sodium-dependent ascorbate transport activity, QN and QY, do not have substantially higher sodium-independent ascorbate or dehydroascorbate transport activities (Figure 7), indicating no changes in substrate specificity. QH (wild type), QN, and QY had 16–20-fold more sodium-dependent ascorbate transport activity than the sodium-independent ascorbate transport activity. Other mutants with little sodium-dependent ascorbate transport activities showed a ratio of 1–4 for sodium-dependent versus sodium-independent ascorbate transport activity (Figures 4B and 6B vs 7B). Interestingly, although His51Gln (QQ) did not show much sodium-dependent ascorbate transport activity (Figure 4B), it had elevated sodium-independent dehydroascorbate transport activity compared to that of both wild type SVCT1 and other mutants (Figure 7). While wild type hSVCT1 had 10-fold higher sodium-dependent ascorbate transport activity (Figure 4B) compared to that of the sodium-independent dehydroascorbate transport activity (Figure 7), the mutant had 6-fold higher sodium-independent dehydroascorbate transport activity (Figure 7 vs Figure 4B). Gln51 in the QQ mutant, by itself, is not sufficient for the observed increase in dehydroascorbate transport activity as a further mutation of Gln50 in QQ to His50 (HQ) abolished the increase (Figure 7).

Dehydroascorbate was shown previously to be transported by glucose transporters (*2*); therfore, the affinity of glucose for the His51Gln (QQ) mutant was tested. The sodium-independent transport of dehydroascorbate in QQ can be

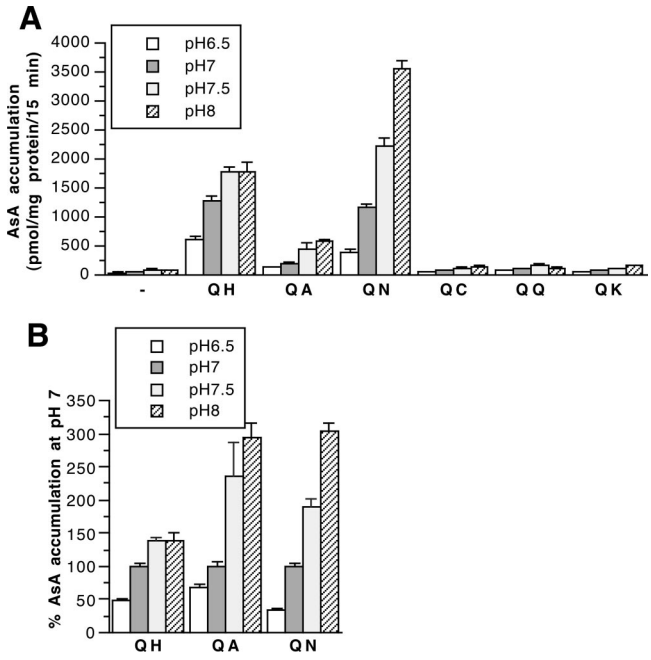

FIGURE 5: pH dependence of sodium-dependent ascorbate uptake by MDCK cells expressing SVCT1 and mutants. (A) Total uptake activity (at 10 μM ascorbate and 135 mM sodium). (B) Uptake activity of each cell type with significant activity normalized by its observed activity at pH 7. -, nontransfected MDCK cells; QH, MDCK cells transfected with wild type SVCT1. Other MDCK cells transfected with mutant SVCT1 are identified by the respective amino acid residue used to substitute for His51. The results are the means ± SD of three independent wells of cells. Some error bars are too small to be visible.

competed significantly by unlabeled dehydroascorbate but not by comparable concentrations of glucose (Figure 8A). Because of the relatively low aqueous solubility of dehydroascorbate, we were not able to test concentrations that would achieve greater than 30% competition of radiolabeled dehydroascorbate uptake. The transport of 2-deoxy-D-glucose and another hydrophobic compound, phenylalanine, was similar between the wild type SVCT1 and QQ mutant (Figures 1S and 2S, Supporting Information). Thus, the specific increase in dehydroascorbate transport into QQ cells suggests that it was likely mediated by the hSVCT1-QQ mutant protein.

The pH dependence of the dehydroascorbate transport activity in the His51Gln (QQ) mutant was determined in Figure 8B. In contrast to the increased sodium-dependent ascorbate transport activity at higher pH as shown in Figure 5, a decrease in the uptake of dehydroascorbate was observed as the buffer pH increased from 6.5 to 8.0. There was no observed precipitation of dehydroascorbate at higher pH during the uptake experiment. Although the loss of activity at higher pH may partly be explained by the instability of dehydroascorbate at higher pH (Figure 8B), the magnitude of the decrease in uptake is greater than that in stability (Figure 8B white bars vs gray bars). The dehydroascorbate transport activity of QQ cells was cation-independent as replacing NMG with Na+, K+, or Li+ had no effect on the activity (Figure 3S, Supporting Information).

DISCUSSION

Stably transfected mutants of EGFP-tagged SVCTs were used to determine the functional significance of conserved histidines in SVCTs. Three potential roles of histidines were examined in this article: membrane localization of SVCTs; the pH dependence of SVCT activity; and ascorbate substrate binding. The first area of interest is whether any of these histidines are absolutely required for the correct membrane localization of SVCTs in MDCK cells. As demonstrated in Figures 2A, 3A, 4A, and 6A, replacing histidines with alanine or other amino acid residues did not affect the predominantly apical or basolateral localization of hSVCT1 or hSVCT2, respectively, compared to that in the wild type. Thus, the data do not support an essential role of these histidines in membrane localization. These data also indicate that overall protein structure was unlikely to be significantly affected in any of the mutants we tested. It has been noted that hydrophobicity generally promotes membrane insertion (*27, 28*), and His51 in hSVCT1 and His109 in hSVCT2 are consistently predicted to be embedded in TM1 (Figure 1) among mostly hydrophobic residues. Thus, even the mutation of His51 to Arg, Lys, Glu, and Asp might not be expected to inhibit membrane insertion since these amino acid residues only have moderately higher biological ΔG^{aa}_{app} relative to His (biological ΔG^{aa}_{app} was calculated by placing the amino acid of interest in the middle of the 19-residue hydrophobic stretch) (*27*). Furthermore, protein–protein interaction is found to promote the partitioning of amino acid side chains into biological lipid bilayers beyond hydrophobicity considerations (*29*).

The second area that we have addressed concerns the role of His51 on the observed pH dependence of sodium-dependent ascorbate transport activity. On the basis of the results in Figure 5, the presence of a histidine residue at position 51 cannot account for the pH dependence of SVCT1. The pH-dependent change in transport activity persisted even after amino acid residues with nonionizable side chains such as A, Q, and N (that cannot sense the pH change) were used to replace histidine. We also found that the conversion of three other conserved histidines to alanines (H147A, H210A, and H354A as characterized in Figure 2) failed to affect the pH dependence of hSVCT1 (Figure 4S, Supporting Information). However, we cannot at present exclude the possibility that multiple histidines may simultaneously contribute to pH sensitivity as has been shown in other proteins (*14*). Alternatively, pH dependence may be governed by nonhistidine residues as the pK_a of an amino acid residue can shift in its protein environment (*30*).

The third area that we investigated relates to the importance of the conserved histidines, specifically His51 in TM1, in ascorbate substrate binding. Proper membrane insertion and polarized sorting of the various mutant proteins (Figures 2A, 3A, 4A, and 6A) indicate that gross perturbations in protein structure have not occurred and thus cannot account for the behavior of the mutant hSVCTs. Although some variations among mutants in the level of expression are expected, the confocal fluorescence images (Figures 2, 3, 4, and 6) and the measurements of total fluorescence emission from the entire monolayer (Table 1S, Supporting Information) do not support a significant reduction in the expression level of nonfunctional mutants. Instead, our data suggest that a decrease in ascorbate binding affinity is the likely cause, directly or indirectly, of the functional loss observed for hSVCT mutants. The increase in the apparent *K*m of our His51 mutants appears to parallel the loss in activity (Figure

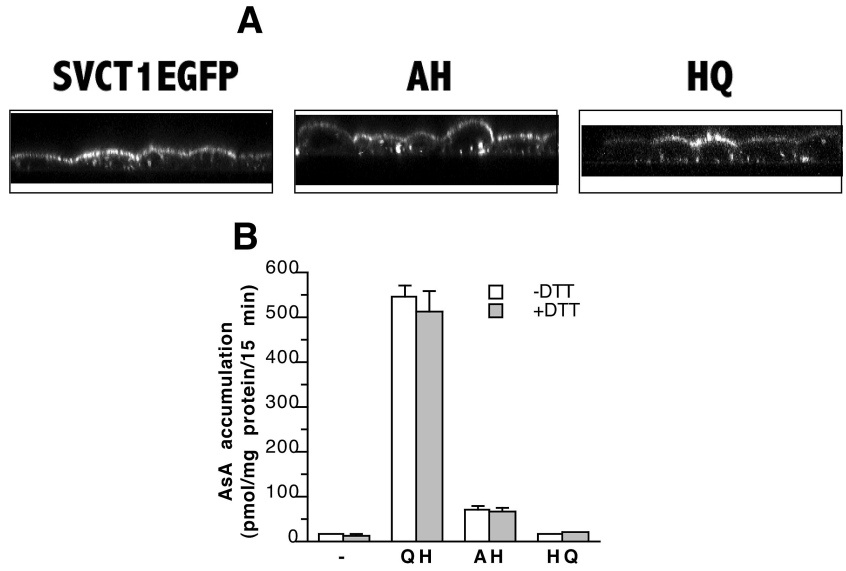

FIGURE 6: Characterization of SVCT1 Gln50 mutants. (A) Apical membrane localization. (B) Net sodium-dependent ascorbate transport activity (at 10 μM ascorbate and 135 mM sodium) in the absence and presence of DTT. -, untransfected MDCK cells; QH, the wild type SVCT1 with Gln50 and His51; AH, substituting Gln50 in SVCT1 with alanine; HQ, reversing QH in SVCT1. Transport activities were measured in three independent wells of cells and are expressed as the means ± SD. Data for MDCK cells and SVCT1 cells were from Figure 4B. Some error bars are too small to be visible.

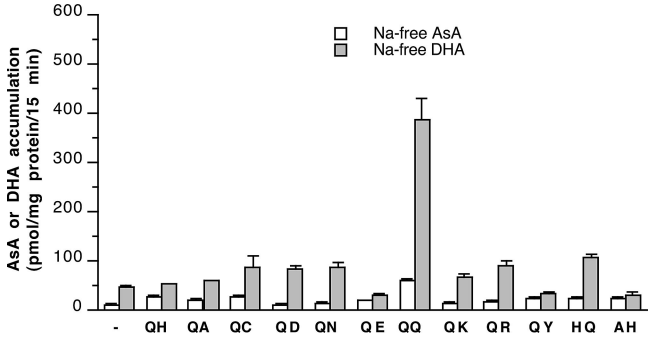

FIGURE 7: Comparison of sodium-independent ascorbate (AsA) and dehydroascorbate (DHA) transport activities in various SVCT1 H51 mutants. The transport activity was measured in sodium-free buffer containing 10 μM substrate and 135 mM NMG in place of sodium. -, nontransfected MDCK cells; QH, MDCK cells transfected with wild type SVCT1. Other bars represent measurements derived from MDCK cells transfected with mutant SVCT1 with the corresponding amino acid substitution. The results are the means ± SD of three independent wells of cells. Some error bars are too small to be visible. All experiments were carried out in the same passage of cells as those in the data shown in Figures 4B and 6B.

4B). The effect of mutation on *V*max, however, is minimal. The two amino acids, Asn and Tyr, that were able to support partial activities can hydrogen bond and are uncharged while Tyr also has a ring similarly planar to that of His. The importance of the hydrogen bond is further supported by the observed low activity in His51Ala (QA). The low activity of His51Asp (QD) relative to QN (Figure 4B) could be the result of the charge. A deleterious effect of charge is supported by the observation of three other mutants with little transport activities, His51Glu (QE), His51Arg (QR), and His51Lys (QK) (Figure 4B). Our His51Gln (QQ) mutant also had little sodium-dependent vitamin C transport activity (Figure 4B). Although the side chain of Gln is uncharged and can hydrogen bond, compared to the side chains of His, Asn and Tyr, it appears to be more flexible and thus bulky. Changes in the amino acid side chains in various mutants are likely to induce minor protein structure change locally and thus perturb the sodium-dependent vitamin C transport.

Another finding that is consistent with a role of His51 in ascorbate substrate binding is the specific increase in sodium-independent dehydroascorbate permeability and thus a change in the substrate specificity of the QQ mutant of hSVCT1 (Figure 7). The nearly complete loss of activity when the adjacent Gln50 residue was mutated as in the case of AH and HQ (Figure 6B), although it cannot specifically support the substrate binding role of His51, provides ancillary information on the essential nature of His51 and more broadly, TM1, in sodium-dependent vitamin C transport. The predicted location of His51 in the middle of the lipid bilayer (Figure 1) would not contradict its proposed importance in substrate binding as substrate binding sites have been found, through crystal structure analysis, within the membrane bilayer in the bacterial protein LeuT, a bacterial homologue of the mammalian Na^+/Cl^--dependent neurotransmitter transporters (*31*).

Our data also provide limited information on the possible biochemical role of His51. The imidazole nitrogen of His205 in *Lac* permease was proposed to play a critical role in hydrogen bond formation (*32*). On the basis of the activity profile of the mutants that we tested (Figure 4B), His51 in hSVCT1 is likely to play a similar role. The two mutants that have substantial activities, QY and QN, have polar but uncharged side chains, while the two mutants that bore positively charged side chains, QK and QR, similar to the His205Arg mutation in *Lac* permease (*32*), have no transport activity. A tyrosine mutation was also found to have partial function when replacing histidine in another membrane transporter (*14*). Indeed, tyrosine and asparagine have been found to be two most common substitutions for histidine residues in homologous proteins (BLOSUM62 matrix www.NCBI.nlm.nih.gov/Class/Structure/aa/aa_explorer.cgi). As was seen in hSVCT1, Gln was shown to be a poor His substitute compared to that of Asn in an unrelated protein

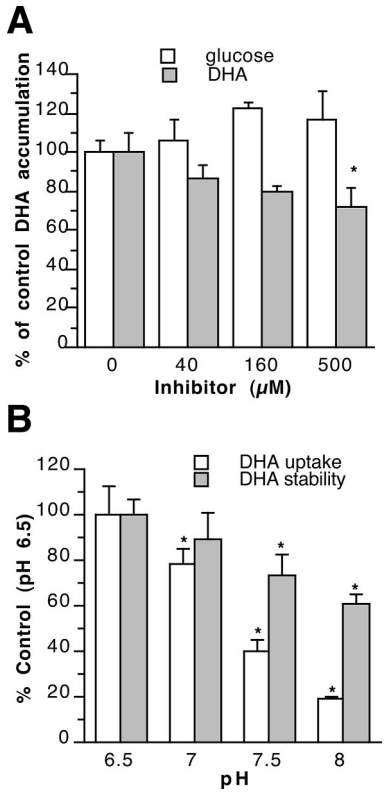

FIGURE 8: Characterization of the increased sodium-independent dehydroascorbate (DHA) uptake by MDCK cells expressing the QQ mutant (His51 to Gln51) of hSVCT1. (A) Dose-dependent inhibition of 10 μM ^{14}C-DHA uptake by unlabeled DHA but not by glucose. Transport activity was measured in sodium-free buffer that contained 135 mM NMG to replace sodium. One-Way ANOVA found a significant effect of dehydroascorbate but not glucose on transport activity. *, significantly different from the control (no additional DHA). (B) The pH dependence of sodium-independent dehydroascorbate uptake by MDCK cells expressing the QQ mutant of SVCT1 and the pH dependence of dehydroascorbate stability. Transport activity and stability were both measured in sodium-free buffer that used 135 mM NMG in place of sodium. The results are the means ± SD of three independent wells of cells or three independent tubes. One-Way ANOVA was performed to determine the effect of pH on uptake or stability. *, significantly different from the observation at pH 6.5.

(*33*). In that case, the utilization of π-N in His for the hydrogen bond partner was proposed as an explanation of the disparity.

In conclusion, kinetic and substrate specificity analyses from this article suggest a direct or indirect role of the conserved histidine in TM1 of hSVCT1 in the ascorbate substrate binding and transport activity. The overall importance of TM1 in hSVCTs is further supported by a loss of function of the corresponding His109Ala mutation in hSVCT2 and the loss of activity of mutations that targeted adjacent Gln50. Our data provide some new insight in predicting the structure–function relationships of this group of membrane proteins.

ACKNOWLEDGMENT

We appreciate the technical guidance of Dr. Wade Sigurdson, Director of Confocal and 3-D Imaging Facility in University at Buffalo. We are also indebted to the critical comments of Dr. Kenneth M. Blumenthal, Dr. Murray J. Ettinger, Dr. Michael D. Garrick, Dr. Daniel J. Kosman, and Dr. Mark D. Sutton of the Department of Biochemistry, University at Buffalo during data analysis and manuscript preparation.

SUPPORTING INFORMATION AVAILABLE

Total fluorescence emission from monolayers of various cell lines is listed in the Supporting Information Table 1S. Additional transport activity characterizations of various mutant cell lines are included in Supporting Information Figures 1S–4S. This material is available free of charge via the Internet at http://pubs.acs.org.

REFERENCES

1. Takanaga, H., MacKenzie, B., and Hediger, M. A. (2004) Sodium-dependent ascorbic acid transporter family SLC23. *Pflugers Arch. 447*, 677–682.
2. Wilson, J. (2005) Regulation of vitamin C transport. *Annu. Rev. Nutr. 25*, 105–125.
3. Sotiriou, S., Gispert, S., Cheng, J., Wang, Y., Chen, A., Hoogstraten-Miller, S., Miller, G. F., Kwon, O., Levine, M., Guttentag, S. H., and Nussbaum, R. L. (2002) Ascorbic acid transporter Slc23a1 is essential for vitamin C transport into the brain and for perinatal survival. *Nature Med. 8*, 514–517.
4. Erichsen, H., Engel, S., Eck, P., Welch, R., Yeager, M., Levine, M., Siega-Riz, A., Olshan, A., and Chanock, S. (2006) Genetic variation in the sodium-dependent vitamin C transporters, SLC23A1, and SLC23A2 and risk for preterm delivery. *Am. J. Epidemiol. 163*, 245–254.
5. Savini, I., Rossi, A., Pierro, C., Avigliano, L., and Catani, M. (2007) SVCT1 and SVCT2: key proteins for vitamin C uptake, Amino Acids [Online early access], DOI 10.1007/s00726-007-0555-7.
6. Boyer, J. C., Campbell, C. E., Sigurdson, W. J., and Kuo, S.-M. (2005) Polarized localization of vitamin C transporters, SVCT1 and SVCT2, in epithelial cells. *Biochem. Biophys. Res. Commun. 334*, 150–156.
7. Subramanian, V. S., Marchant, J. S., Boulware, M. J., and Said, H. M. (2004) A carboxy-terminal region dictates the apical plasma membrane targeting of the human sodium-dependent vitamin C transporter-1 in polarized epithelia. *J. Biol. Chem. 279*, 27719–27728.
8. Kuo, S.-M., MacLean, M. E., McCormick, K., and Wilson, J. X. (2004) Gender and sodium-ascorbate transporter isoforms determine ascorbate concentrations in mice. *J. Nutr. 134*, 2216–2221.
9. Poolman, B., Modderman, R., and Reizer, J. (1992) Lactose transport system of Streptococcus thermophilus. The role of histidine residues. *J. Biol. Chem. 267*, 9150–9157.
10. He, M., and Kaback, H. (1997) Interaction between residues Glu269 (helix VIII) and His322 (helix X) of the lactose permease of Escherichia coli is essential for substrate binding. *Biochemistry 36*, 13688–13692.
11. Fujisawa, Y., Tateoka, R., Nara, T., Kamo, N., Taira, T., and Miyauchi, S. (2006) The extracellular pH dependency of transport activity by human oligopeptide transporter 1 (hPEPT1) expressed stably in Chinese hamster ovary (CHO) cells: a reason for the bell-shaped activity versus pH. *Biol. Pharm. Bull. 29*, 997–1005.
12. Ek, J., Delmar, M., Perzova, R., and Taffet, S. M. (1994) Role of histidine 95 on pH gating of the cardiac gap junction protein connexin43. *Circ. Res. 74*, 1058–1064.
13. Zong, X., Stieber, J., Ludwig, A., Hofmann, F., and Biel, M. (2001) A single histidine residue determines the pH sensitivity of the pacemaker channel HCN2. *J. Biol. Chem. 276*, 6313–6319.
14. Stewart, A. K., Kurschat, C. E., Burns, D., Banger, N., Vaughan-Jones, R. D., and Alper, S. L. (2007) Transmembrane domain histidines contribute to regulation of AE2-mediated anion exchange by pH. *Am. J. Physiol. Cell Physiol. 292*, C909–918.
15. Malo, C., and Wilson, J. X. (2000) Glucose modulates vitamin C transport in adult human small intestinal brush border membrane vesicles. *J. Nutr. 130*, 63–69.
16. Liang, W. J., Johnson, D., and Jarvis, S. M. (2001) Vitamin C transport systems of mammalian cells. *Mol. Membr. Biol. 18*, 87–95.
17. Loffing-Cueni, D., Loffing, J., Shaw, C., Taplin, A., Govindan, M., Stanton, C., and Stanton, B. (2001) Trafficking of GFP-tagged DeltaF508-CFTR to the plasma membrane in a polarized epithelial cell line. *Am. J. Physiol. Cell Physiol. 281*, C1889–1897.

18. Grati, M., Aggarwal, N., Strehler, E., and Wenthold, R. (2006) Molecular determinants for differential membrane trafficking of PMCA1 and PMCA2 in mammalian hair cells. *J. Cell Sci. 119*, 2995–3007.
19. Hatanaka, T., Hatanaka, Y., Tsuchida, J., Ganapathy, V., and Setou, M. (2006) Amino acid transporter ATA2 is stored at the trans-Golgi network and released by insulin stimulus in adipocytes. *J. Biol. Chem. 281*, 39273–39284.
20. Kuo, S.-M., Morehouse, H. F. J., and Lin, C.-P. (1997) Effect of antiproliferative flavonoids on ascorbic acid accumulation in human colon adenocarcinoma cells. *Cancer Lett. 116*, 131–137.
21. Kuo, S.-M., and Lin, C. P. (1998) 17β-estradiol inhibition of ascorbic acid accumulation in human intestinal Caco-2 cells. *Eur. J. Pharmacol. 361*, 253–259.
22. Mawatari, S., and Murakami, K. (2001) Effects of ascorbate on membrane phospholipids and tocopherols of intact erythrocytes during peroxidation by t-butylhydroperoxide: comparison with effects of dithiothreitol. *Lipids 36*, 57–65.
23. Kuo, S.-M., Tan, D., and Boyer, J. C. (2004) Cellular vitamin C accumulation in the presence of copper. *Biol. Trace Elem. Res. 100*, 125–136.
24. Roe, J. H., and Kuether, C. A. (1943) The determination of ascorbic acid in whole blood and urine through the 2,4-dinitrophenylhydrazine derivative of dehydroascorbic acid. *J. Biol. Chem. 147*, 399–407.
25. Peterson, G. L. (1983) Determination of total protein. *Methods Enzymol. 91*, 95–119.
26. Tsukaguchi, H., Tokui, T., Mackenzie, B., Berger, U. V., Chen, X. Z., Wang, Y., Brubaker, R. F., and Hediger, M. A. (1999) A family of mammalian Na+-dependent L-ascorbic acid transporters. *Nature 399*, 70–75.
27. Hessa, T., Kim, H., Bihlmaier, K., Lundin, C., Boekel, J., Andersson, H., Nilsson, I., White, S. H., and von Heijne, G. (2005) Recognition of transmembrane helices by the endoplasmic reticulum translocon. *Nature 433*, 377–381.
28. Hessa, T., White, S. H., and Von Heijne, G. (2005) Membrane insertion of a potassium-channel voltage sensor. *Science 307*, 1427.
29. MacCallum, J., Bennett, W., and Tieleman, D. (2007) Partitioning of amino acid side chains into lipid bilayers: results from computer simulations and comparison to experiment. *J. Gen. Physiol. 129*, 371–377.
30. Cederholm, M., Stuckey, J., Doscher, M., and Lee, L. (1991) Histidine pKa shifts accompanying the inactivating Asp121-Asn substitution in a semisynthetic bovine pancreatic ribonuclease. *Proc Natl Acad Sci U S A 88*, 8116–8120.
31. Yamashita, A., Singh, S., Kawate, T., Jin, Y., and Gouaux, E. (2005) Crystal structure of a bacterial homologue of Na+/Cl–dependent neurotransmitter transporters. *Nature 437*, 215–223.
32. Puttner, I., Sarkar, H., Poonian, M., and Kaback, H. (1986) lac permease of Escherichia coli: histidine-205 and histidine-322 play different roles in lactose/H+ symport. *Biochemistry 25*, 4483–4485.
33. Lowe, D., Fersht, A., Wilkinson, A., Carter, P., and Winter, G. (1985) Probing histidine-substrate interactions in tyrosyl-tRNA synthetase using asparagine and glutamine replacements. *Biochemistry 24*, 5106–5109.

BI701666Q